Experimental Mechanics (2006) 46: 257–268
DOI 10.1007/s11340-006-6067-7

Effects of Environmental Degradation on Flexural Failure Strength of Fiber Reinforced Composites

T. Nakamura · R.P. Singh · P. Vaddadi

Received: 11 August 2005 / Accepted: 7 November 2005 / Published online: 22 February 2006

Abstract Fiber-reinforced composite laminates are often used in harsh environments that may affect their long-term durability as well as residual strength. In general, environmental degradation is observed as matrix cracking and erosion that leads to deterioration of matrix-dominated properties. In this work, cross-ply laminates of carbon fiber reinforced epoxy were subjected to environmental degradation using controlled ultraviolet radiation (UV) and moisture condensation and the post-exposure mechanical properties were evaluated through elastic modulus and failure strength measurements. Additionally, both degraded and undegraded were subjected to cyclic fatigue loading to investigate possible synergistic effects between environmental degradation and mechanical fatigue. Experimental results show that the degradation results in reduced failure strength. Greater effects of degradation are observed when the materials are tested under flexural as opposed to uniaxial loading. Based on strength measurements and scanning electron microscopy, we identified various damage modes resulting from exposure to UV radiation and moisture condensation, and cyclic loading. The principal mechanisms that lead to reduction in mechanical properties are the loss of fiber confinement due to matrix erosion, due to UV radiation and moisture condensation, and weakened/cracked ply interfaces due to mechanical fatigue. An empirical relationship was established to quantify the specific influence of different damage mechanisms and to clarify the effects of various degradation conditions.

Keywords Composites · Environmental degradation · UV radiation · Moisture · Fatigue · Residual strength

T. Nakamura (✉) · R.P. Singh (SEM member) · P. Vaddadi
Department of Mechanical Engineering,
State University of New York at Stony Brook,
NY 11794, USA
e-mail: toshio.nakamura@sunysb.edu

Introduction

Fiber reinforced composites offer significant advantage over traditional materials. However, composites are susceptible to degradation by moisture, temperature, ultraviolet (UV) radiation, thermal cycling and mechanical fatigue. For example, when exposed to humid environments, carbon-epoxy composites absorb moisture, which leads to changes in the thermophysical, mechanical and chemical characteristics of the epoxy matrix by plasticization and hydrolysis [1–3]. These changes in polymer structure can lower both the elastic modulus and the glass transition temperature [4–6]. Furthermore, moisture absorption induced dilatational expansion can also cause irreversible damage at the fiber-matrix interface and along interlaminar boundaries due to material property mismatch. For the increased reliability and durability of these materials, their capacity for sustained performance under harsh and changing environmental conditions must be quantified. A recent study [7] examined the physical, chemical and mechanical degradation of an IM7/997 carbon fiber reinforced epoxy composite following exposure to UV radiation and/or water vapor condensation. Based on observations of physical and chemical degradation, it was concluded that these two environments operate in a synergistic manner, which causes severe microcracking and erosion of the epoxy matrix.

Composite structures are often subject to various environments as well as repeated mechanical loading. For example, fatigue by cyclic load is an inherent issue in rotating components such as rotor blades for helicopters and wind turbines that are also exposed to various environmental conditions. Furthermore, failure due to cyclic loading is by far the most common type of in-service failure observed for composite materials [8]. Thus it would be valuable to understand combined effects of environmental conditions and cyclic loading. Damage accumulation during cyclic loading is significantly more complex in composites than in metals or ceramics. The complex internal microstructure of composite materials introduces various modes of damage such as delamination, matrix cracking, debonding, ply failure and fiber breakage. These damage modes may act in concert with one another to produce a collective result. Often the damage accumulation process is characterized by the initiation of numerous small cracks rather than the propagation of a dominant crack, as observed for metals. Finally, the particular fatigue response of a composite, under a given loading condition, depends on the properties of each ply and the stacking sequence [9, 10]. Challenges in studying the fatigue of composites are magnified when environmental degradation is also taken into account. Environmental exposure leads to physical/chemical degradation that affects the baseline material properties and can also provide localized damage initiation sites for damage accumulation under fatigue loading. As a first step towards understanding these effects, this study is focused on the fatigue response of composites that have been pre-exposed to environmental degradation conditions, viz. UV radiation and moisture condensation. Changes in elastic moduli as well as the residual strength are measured and investigated. Our objective is to better estimate composite integrity and durability under accelerated aging environments through the identification of basic underlying failure mechanisms. It should also be noted that while significant research has been focused towards understanding the effects of the hygrothermal aging on fatigue response of composites, similar investigations which also account for exposure to UV radiation and mechanical fatigue are non-existent.

Experimental Procedure

Material and Specimen Description

The effects of various degradation mechanisms were investigated on the IM7/997 carbon fiber reinforced epoxy composite. This composite is under development and qualification for application to aerospace and rotorcraft structures and is expected to provide higher damage tolerance than currently qualified materials such as IM7/5271-1 [11]. Specimens with dimensions of 152 × 12 × 1.2 mm were prepared from $[0/90]_{2S}$ laminates of IM7/997 provided by Cytec Engineered Materials (Anaheim, CA). Figure 1 shows a schematic representation of the cross-ply composite laminate. The fiber volume fraction was determined to be 58 ± 1% based on image analysis of polished cross-sections. The specimens were machined using a high-speed diamond saw, with water used as coolant to minimize cutting damage. Specimen edges were then polished using 120, 400 and 600 grit metallographic papers to remove any surface damage, which might have been introduced during the machining process. The cut and polished specimens were then stored in a desiccator at ambient temperature typically for one to two weeks prior to subjecting them to any environmental exposure condition.

Environmental Exposure Conditions

Various exposure conditions were imposed upon the specimens in a QUV/Se weathering chamber (Q-Panel Lab Products, Cleveland, Ohio). The QUV/Se reproduces accelerated conditions by sunlight, rain and dew by exposing materials to controlled cycles of UV radiation and water vapor condensation. The UV radiation is generated by fluorescent lamps that simulate the UV component of solar radiation in the 295–365 nm wavelength range. The intensity of UV radiation is continuously monitored and controlled by four irradiance detectors. Water condensation is provided by the generation of vapor from a water bath. This condenses on the specimen surface and thereby simulates rain and dew. The IM7/997 $[0/90]_{2S}$ specimens were subjected to three different environmental exposure conditions, as summarized in Table 1: (a) 500 hours of

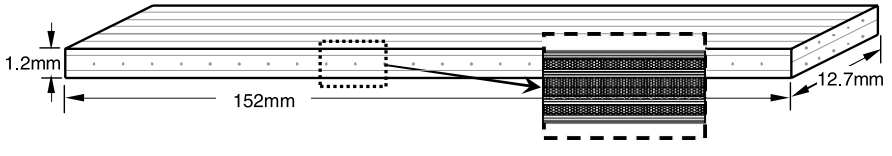

Fig. 1. Schematic representation of the $[0/90]_{2S}$ carbon fiber-reinforced crossply composite laminate

Table 1 Specifications of the different environmental conditions

Environmental condition	Test specifications
500 hours UV radiation	Irradiance level of 0.68 W/m^2 at 340 nm and T = 60°C
500 hours condensation	Condensation at T = 50°C and 100% relative humidity
1000 hr cyclic exposure	Repeated UV radiation and condensation in 6 hr cycle

continuous UV radiation, (b) 500 hours of continuous vapor condensation and (c) 1000 hours of exposure to alternating UV radiation and vapor condensation using a 6 hour repeat cycle. In the last exposure, the specimens were exposed to alternating cycles consisting of 6 hours of UV radiation followed by 6 hours of condensation. This combined exposure condition was selected based on our earlier investigations that have demonstrated synergistic effects of the two environmental conditions [7].

Cyclic Loading

Uniaxial tension-tension cyclic loading tests were performed on specimens that had been subjected to different environmental exposure conditions to investigate the mechanical fatigue response. The test were conducted under three different maximum load levels, f = 0.25, 0.50 and 0.75, using the load-controlled mode on a servo-hydraulic universal testing machine in accordance with the relevant ASTM standard [12]. Here f denotes the maximum applied load P_{max} normalized by the ultimate tensile strength (UTS) of an undegraded and non-fatigued $[0/90]_{2S}$ specimen. The minimum to maximum load ratio (i.e., $P_{\min}$ / $P_{\max}$), was set to 0.1 and the loading frequency was kept at 5 Hz to minimize hysteresis induced heating. All the specimens were fatigued for 100,000 cycles and the real-time change in elastic modulus during fatigue was measured using an extensometer attached to a specimen [13]. Typical variations of the longitudinal moduli during the cyclic loading of specimens that were pre-exposed to 500 hours of moisture condensation is shown in Fig. 2 for the three different fatigue load levels. In general, a gradual increase in the modulus was observed for low amplitude fatigue (f = 0.25) while the modulus tended to decrease under high amplitude fatigue (f = 0.25).

After mechanical fatiguing the specimens were subjected to three-point-bend tests to measure the net change in flexural modulus. Table 2 lists the net change in uniaxial and flexural moduli. Essentially, the modulus drop was greater for specimens subjected to environmental degradation and higher amplitudes of cyclic loading. For all specimens subjected to low amplitude fatigue (f = 0.25) a slight increase in modulus was observed as compared to specimens that were not subjected to fatigue. This highly counter-intuitive observation was validated by repeated testing and by using strain gage measurements both during and at the end of fatigue loading. At first, this phenomenon was thought to occur simply due to the re-alignment of misaligned fibers. However the straightening of fibers could not have generated the observed ~10% increase. Furthermore, we had not observed a similar behavior for uniaxial $[0]_8$ laminates. Thus it appears the source of increase in elastic modulus could be due to the release of residual deformation/stresses along the cross ply boundaries. It is also worth noting that elastic modulus of 85 GPa measured for un-degraded specimens that were fatigue at f = 0.25 specimen is very close to the value estimated by the rule-of-mixture using the constituent properties and fiber volume fraction.

Surface Morphology of Damaged Specimen

Various damage phenomena can be observed in the SEM micrographs shown in Fig. 3. A major visible damage due to the environmental degradation by UV radiation and moisture condensation is the matrix erosion as shown in Fig. 3(a). Here the matrix erosion is clearly visible in the 90° ply. Internal matrix cracking is also observed in this micrograph. The mechanically fatigued specimen without environmental degradation shows long transverse cracks in the 90° ply, as shown in Fig. 3(b). Without surface erosion by UV radiation and moisture condensation, other effects are not visible from this micrograph. However more details can be observed in specimens subjected to combined environ-

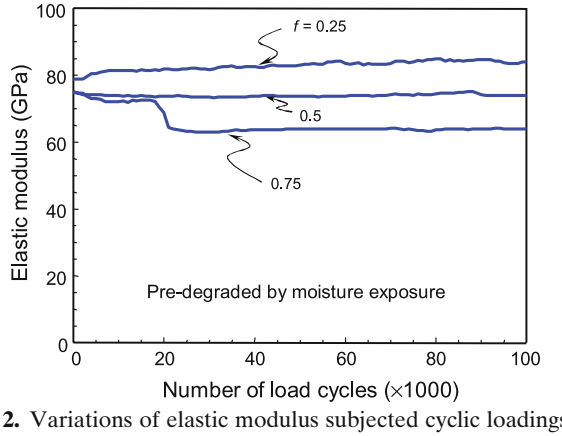

Fig. 2. Variations of elastic modulus subjected cyclic loadings at various load amplitude

Table 2 Measured effective modulus under uniaxial tension and flexural load after environmental degradations and cyclic load fatigue

	Undegraded	UV	Moisture	UV-moisture
Uniaxial modulus of uniaxial plies without fatigue (GPa)				
Ply sequence				
$[0]_8$	156 ± 4	154 ± 1 (−1%)	154 ± 1 (−1%)	155 ± 1 (1%)
$[90]_8$	9.9 ± 1	9.2 ± 1 (−6%)	9.6 ± 1 (−2%)	9.5 ± 1 (−4%)
Uniaxial modulus of cross-ply $[0/90]_{2s}$ with fatigue (GPa)				
Fatigue level				
0	78 ± 2	78 ± 1 (0%)	76 ± 1 (−2%)	74 ± 1 (−5%)
0.25	85 ± 1 (9%)	86 ± 2 (10%)	84 ± 2 (8%)	79 ± 2 (−1%)
0.50	72 ± 2 (−8%)	74 ± 1 (−5%)	74 ± 1 (−5%)	72 ± 1 (−8%)
0.75	73 ± 1 (−7%)	66 ± 1 (−15%)	64 ± 2 (−18%)	58 ± 1 (−26%)
Flexural modulus of cross ply $[0/90]_{2s}$ with fatigue under three-point-bend (GPa)				
Fatigue level				
0	73 ± 1	72 ± 1 (−1%)	72 ± 1 (−1%)	75 ± 1 (−11%)
0.25	78 ± 1 (7%)	76 ± 2 (4%)	73 ± 2 (0%)	69 ± 2 (−5%)
0.50	70 ± 2 (−4%)	70 ± 1 (−4%)	70 ± 1 (−4%)	66 ± 1 (−10%)
0.75	69 ± 1 (−5%)	68 ± 1 (−7%)	68 ± 1 (−7%)	61 ± 1 (−16%)

The results are the average of two specimens with spread shown. Relative changes as respect to virgin specimens are noted in parentheses

mental degradation and fatigue loading. Figures 3(c) and (d) show the cross section of a specimen that was exposed to alternating UV radiation and moisture condensation, and then subjected to fatigue loading at $f = 0.75$. Fiber breakage as well as interface debonding between 0° and 90° plies is clearly evident. In fact the delamination crack can be quite long, as shown in Fig. 3(d). The synergistic effects of UV radiation and condensation lead to significant material deterioration which accelerates damage accumulation under cyclic load fatigue. In addition, although not visible from the micrographs, it is possible that there may be substantial fiber-matrix debonding, which can lead to reduction in residual strength.

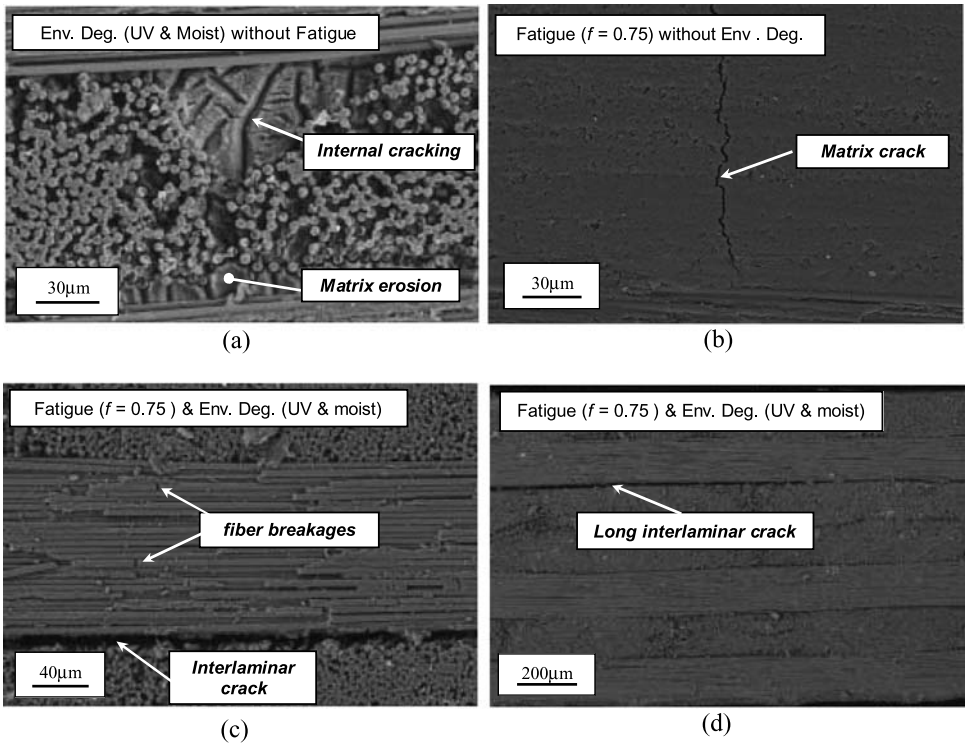

Fig. 3. SEM micrographs of various specimen showing different types of damages. (**a**) Only environmental degradation by moisture and UV. (b) Only mechanical fatigue at $f = 0.75$. (**c**) & (**d**) Combined mechanical fatigue ($f = 0.75$) and environmental degradation (moisture and UV)

Classifications of Various Damage Modes

Environmental Degradation

Based on current observations and past studies on environmental degradation of composites, exposure to UV radiation and moisture condensation can generate various modes of damage. UV radiation induces photochemical reactions in the polymeric matrix leading to embrittlement and microcracking, which enhances loss of fiber confinement during mechanical fatigue. Moisture absorption leads to dilatational expansion and also chemical changes such as plasticization and hydrolysis. When these composites are exposed to alternative UV radiation and moisture condensation, synergistic mechanisms lead to material removal in the form of matrix erosion [7]. This is a major damage mode, unique to combined exposure in which moisture condensation washes away the water-soluble products of UV initiated photochemical reactions. While material erosion is limited to the surface layers, this can produce significantly adverse effects on the modulus and strength, especially under flexural loading. These factors are discussed in later sections.

Mechanical Damage

Mechanical loading can cause direct damage to composites, e.g., impact loading may cause fiber breakage as well as cracking. This investigation considers the type of damage that result from cyclic loading when the maximum load level is less than the ultimate failure strength. The fatigue loading of composites at load amplitudes less than one-third of the ultimate strength load has received only limited attention it has been shown that only minimal damage accumulation occurs as long as the duration of loading is long. Furthermore, our own investigation shows that at fatigue load amplitudes of one-quarter of the ultimate load the composite may exhibit a counterintuitive increase in modulus. Once the fatigue the load level reaches about half of the ultimate load, various damage modes start to appear, such as fiber breakage, matrix cracking and interlaminar decohesion. The quantitative effects of various damage modes are described next.

Consequences of Various Types of Damage

Although our composites were subjected to different type of environmental and mechanical degradation resulting in a host of damage types, the individual effects are examined first.

Matrix erosion

The loss of near surface polymeric matrix occurs under combined exposure to alternating UV radiation and moisture condensation. The depth for 1000 hours of combined exposure was observed to be 15–30 μm, which is ~1–3% of the original laminate thickness. At first it was presumed that these losses in the epoxy matrix were too small to have any effect on the overall mechanical characteristics of composites since most of the load is borne by the carbon fibers. However, the matrix is responsible for load transfer to the fibers, and this erosion will lead to a lack of fiber confinement, especially under flexure as shown in Fig. 4(a). Assuming these loose fibers do not contribute to any stiffness of the composite, their effects can be approximated as surface thinning. The resulting decrease in flexure modulus due to surface thinning can be determined using laminate theory and is shown in Fig. 4(b) for the case of our $[0/90]_{2S}$ composite. It suggests that, for say 3% thinning, there is a 13% decrease in flexure modulus, which is very close to the experimental observation of 11% listed in Table 2. It is worth noting that the reduction in fiber-matrix load transfer due to a loss of the matrix phase can lead to detrimental effects even under tensile loading conditions.

Fiber breakage

Limited fiber breakage was observed using scanning electron microscopy for fatigue loading amplitudes of

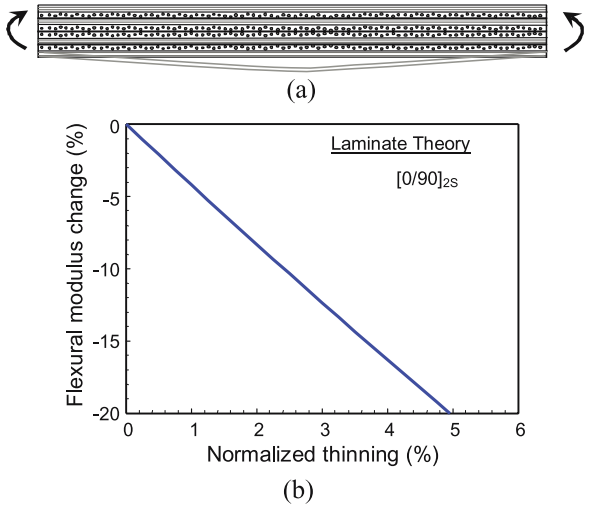

Fig. 4. (**a**) Schematic of loose fibers under bending. (**b**) Drop in flexural modulus shown for equivalent thinning of surfaces of composites

$f = 0.5$. The amount of breakage increased substantially for fatigue loading at higher loads of $f = 0.75$. Fiber breakage leads to disruption in the load transfer path along the loading direction and thus directly to a decrease in the effective modulus. Since in our $[0/90]_{2S}$ composites loaded under tension, the majority of load is carried by the fibers in 0° ply, the breaking of these fibers directly leads to a measurable decrease in the effective modulus. In fact, the relative amount of fiber breakage is directly proportional to the decrease in modulus, e.g., 5% fiber breakage leads to 5% decrease in modulus. Thus, the loss of load transfer can occur either through the matrix erosion as described previously or through the loss of fiber-matrix debonding and fiber breakage during cyclic load. While environmental degradation may also promote fiber-matrix decohesion the exact nature of this mechanism is not clear at the moment.

Matrix cracking

Various types of matrix cracks were observed using scanning electron microscopy. Some long cracks were observed in 90° plies, as shown in Fig. 3(b). Due to surface matrix erosion, these long cracks were not clearly observed clearly in the case of specimens degraded by UV radiation and moisture condensation, but are expected to be present in all specimens fatigued at $f \geq 0.5$. Although the direct effect of these long inter-ply cracks is unclear, they appear to be substantially deep and may promote interlaminate decohesion.

Interlaminar decohesion

Specimens fatigued at $f = 0.75$ exhibited extensive lengthy delamination between plies, as shown in Fig. 3(d). Some of these were longer than several multiples of laminate thickness. Mechanically, the presence of these delaminations will have very little influence on the tensile modulus. However, they can significantly affect the flexural modulus significantly. A finite element model was used to determine the effective flexural stiffness of composite laminates containing a center through-crack between the seventh and eighth plies (interface of 90° and 0° plies) and the results are plotted in Fig. 5(a). Other delamination locations as well as multiple crack geometries were also analyzed and resulted in qualitatively similar observations. The computations predict a sudden decrease in the flexural modulus once the delamination becomes more that 20% of the specimen length. The detrimental effect of delamination is not limited to the flexural modulus. A detailed analysis of the finite element results revealed large changes in the stress state due to the delamination. These occur not near the crack tips where usual stress concentrations exist, but at the middle location of delamination crack, which is significantly away from the tips. The normal and axial stresses in the 90° and 0° plies were computed at locations on either side of the delamination crack under flexural loading. They were averaged in each ply and normalized with respect to the stress state of a no-crack model. As shown in Fig. 5(b), the axial stress increases in seventh ply (90°) and decreases in the eighth ply (0°) in the presence of a delamination. These results have an important implication in failure under flexural loading. In such tests the failure always initiated in the seventh (90°) ply regardless of any previous damage. This suggests that if a crack exists between seventh and eighth plies, it is likely to lower the failure load with a larger stress in the seventh ply. This is further discussed in Section 4. As described above, the different modes of damage accumulation in the composite can lead to changes in various physical states, as summarized in Fig. 6.

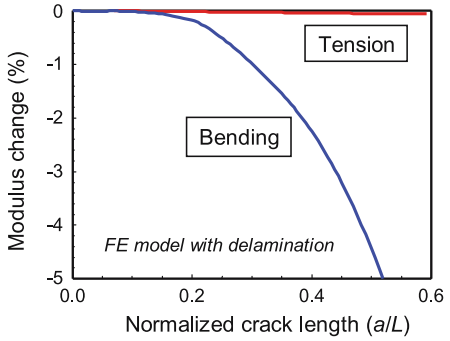

(a)

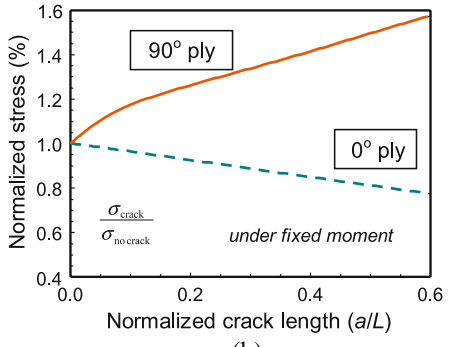

(b)

Fig. 5. (**a**) Normalized change in elastic modulus due to delamination is shown for bending and tensile load. (**b**) Stress changes in 7th (90°) and 8th (0°) plies due to delamination are shown for bending load

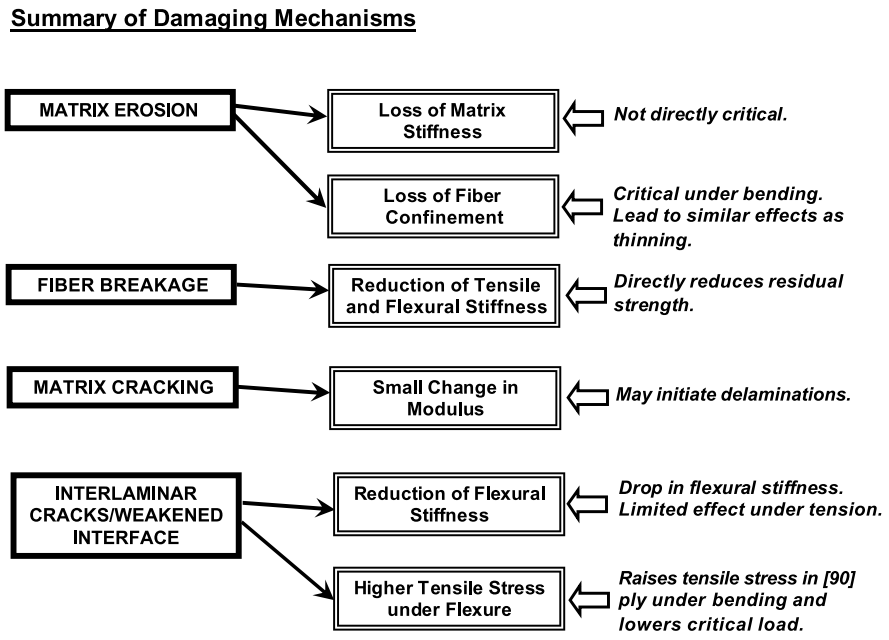

Fig. 6. Summary of possible damage modes in composites subjected to environmental degradations and fatigue load. Possible consequences are noted

Residual Strength Under Flexural Loading

Three-Point-Bend Tests

In order to better understand the synergistic effects of fatigue loading and environmental exposure, the residual strength was measured for each degradation/loading condition under three-point bending. The failure strength was determined in terms of the first-ply failure load. It was observed that failure always occurred in the seventh (90°) ply, which is the second layer from the bottom. Table 3 lists results from the flexure tests for different degradation conditions along with results from previously conducted uniaxial tensile tests. Due to limitations on fatigue loaded specimens and greater difficulties in conducting uniaxial tests, the tensile strength was determined only for specimens subjected to environmental exposure and not fatigue loading. Also, given the large test matrix only two tests were conducted for each condition. While this limits statistical relevance all data was found to be self-consistent and provides a phenomenological basis for our observations.

When composites are not subjected to mechanical fatigue, the environmental conditions have limited influence on the longitudinal tensile strengths of $[0]_8$ and $[0/90]_{2S}$ laminates, as shown in the first part of Table 3. This is expected, since the longitudinal

Table 3 Residual failure loads of composites with various degradations

	Undegraded	UV	Moisture	UV-moisture
Failure stress under uniaxial load for various ply-sequences without fatigue (MPa)				
Ply sequence				
$[0]_8$	2388 ± 59	2432 ± 33 (2%)	2294 ± 50 (−4%)	2320 ± 73 (−3%)
$[90]_8$	61 ± 1	55 ± 3 (−10%)	49 ± 1 (−20%)	44 ± 1 (−27%)
$[0/90]_{2s}$	1270 ± 31	1308 ± 23 (3%)	1220 ± 33 (−4%)	1215 ± 70 (−4%)
Failure moment under three-point-bend of $[0/90]_{2s}$ laminates with fatigue (N·m/m)				
Fatigue level				
0	520 ± 10	441 ± 7 (−15%)	438 ± 4 (−16%)	373 ± 4 (−28%)
0.25	419 ± 7 (−19%)	412 ± 14 (−20%)	402 ± 10 (−22%)	362 ± 8 (−30%)
0.50	384 ± 10 (−26%)	377 ± 7 (−28%)	369 ± 4 (−29%)	355 ± 4 (−31%)
0.75	357 ± 4 (−31%)	348 ± 7 (−33%)	341 ± 7 (−34%)	304 ± 4 (−41%)

First, different ply sequences with various environmental degradations under tension. Second, different fatigue load amplitudes and environmental degradations under flexural load. The values in parentheses are normalized differences with respect to respective undamaged values

properties are governed by the carbon fibers, which are not affected by either UV radiation or moisture condensation. Some slight decrease in properties, observed for the case of UV and combined UV-moisture exposure, is possibly due to surface matrix erosion that makes some fibers unconstrained as described earlier. On the contrary, the degradation of the epoxy matrix resulted in significant deterioration of the tensile strength of $[90]_8$. Specimens exposed to the UV radiation exhibited a 10% decrease, which can be attributed to the microcracks induced by the UV radiation. A decrease of 20% in tensile strength was observed for specimens that were exposed to moisture condensation. The degradation was most severe for specimens that were exposed to both UV radiation and moisture condensation. With combined exposure, the strength decreased by 27% as compared to undegraded specimens.

The second part of Table 3 presents the results from flexural testing. The critical strengths, at the point of first ply failure, are reported in terms of the critical maximum moment per unit thickness occurring at the center of the specimen. As described earlier, the failure always initiated in the 90° ply that was the second layer from the bottom. In the absence of mechanical fatigue ($f = 0$), specimens exposed to both UV radiation and moisture condensation had at the highest failure moment (i.e., greatest strength) followed by the ones exposed to just moisture condensation and then those exposed to only UV radiation. Although this order is consistent with the tensile strength results, the *magnitudes of the changes* are very different. For example, specimens exposed to combined UV radiation and moisture condensation exhibited a 28% decrease in the residual flexural strength as compared to only 4% in the tensile strength. In fact, this decrease was nearly double than that observed for specimens subjected to either UV radiation or moisture condensation along, and it suggests environmental degradation plays a critical role for flexural load conditions. Physically, this large decrease can be only explained by the matrix erosion that occurs on the surface layers, as described earlier.

Furthermore, the residual strengths continued to decline with increasing fatigue load amplitude. For $f = 0.25$ specimens, the trend of changes in flexural failure strength were similar to those observed for $f = 0$. However, it should be noted that the actual magnitude of the flexural strength, for a given environmental exposure condition, was lower for the $f = 0.25$ fatigued samples, as compared to the non-fatigued samples. This was rather unexpected since no surface damage was observed using scanning electron microscopy, and the modulus had actually increased, as listed earlier in Table 2. Since these specimens ($f = 0.25$) are expected to not have any fiber breakage or interlaminar delamination, it is likely that repeated loading caused some damage to matrix as well as matrix-fiber debonding. The latter can disable the load transfer mechanism and lower the failure load without adversely affecting the modulus.

With even larger amplitudes of fatigue load, the failure moments continued to decrease further. For conditions of $f \geq 0.5$, fiber breakage is the additional mode which promotes lowering of residual strength. For $f = 0.75$, many specimens have internal delaminations which can further decrease the strength as described earlier. It is interesting to note the variations were much less for specimens previously exposed to environmental degradations. In fact, for the case of combined UV radiation and moisture condensation, the failure stress changed by only 13% from $f = 0$ to $f = 0.75$ while that for no degradation the decrease was 31% These results suggest that further weakening of specimen due to mechanical fatigue is less pronounced when it has already been weakened by environmental degradation. To better understand and quantify the weakening effects of degradation and fatigue, an empirical formula was constructed.

Empirical Quantification of Failure Stresses

The failure stresses obtained from three-point bend tests were used to quantify residual strengths of composites exposed to the various degradation conditions. Different parameters were defined to account for the individual and coupled effects of the environmental exposure and cyclic loading. The failure stress under flexural load is normalized as $S = S_f / S_f^*$ where S_f is the failure stress of degraded and/or fatigued specimen and S_f^* is the failure stress without any degradation and/or fatigue. In order to establish a meaningful empirical formula, we considered a simple form that will account for both nonlinear as well as coupling effects. Accordingly, the normalized failure stress was assumed to be a quadratic function of amplitude of cyclic load,

$$S = s_1(E_U, E_C) + s_2(E_U, E_C)\, f + s_3(E_U, E_C)\, f^2 \qquad (1)$$

Here s_1, s_2, s_3 are functions that depend on the effects of UV radiation (E_U) and moisture condensation (E_C). Also f is the amplitude of fatigue loading as previously

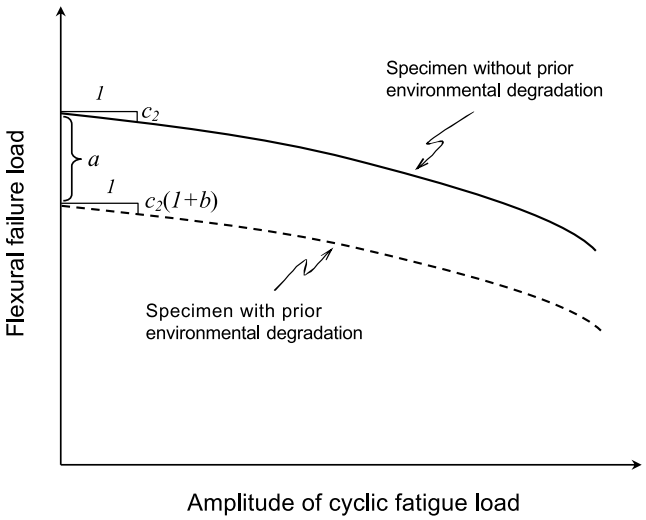

Fig. 7. Roles of parameters in the empirical equation for residual flexural strength are schematically illustrated. Here, parameter *a* represents the decrease of failure load due to environmental exposure without fatigue by cyclic load and the parameter *b* influences the slope of failure load

defined. As a first order approximation, the following functional forms are assumed for s_1, s_2 and s_3,

$$s_1 = (1+a)c_1,\ s_2 = (1+b)c_2 \text{ and } s_3 = c_3. \tag{2}$$

Here c_1, c_2 and c_3 are the constants that essentially fit the quadratic equation for specimens without prior environmental degradation. Also, *a* represents the effects of UV radiation and/or moisture condensation. They are taken to be zero unless the specimen is subjected to the corresponding degradation condition. Note for specimens with combined environmental degradation, all of the constants are non-zero. The other term, *b* is defined similarly. Physically, the parameter *a* represents the decrease of failure stress due to environmental exposure without cyclic fatigue loading as shown in Fig. 7. A large magnitude of *a* for any given case suggests a greater role of the respective environmental condition. The value of *b* influences the slope of change in failure stress as a function of cyclic loading. When it is positive, an environmentally degraded specimen is more sensitive to the variation of cyclic load amplitude, *f*, while a negative *b* denotes a reduced effect of cyclic loading for environmentally degraded specimens.

There are nine parameters to be defined in the proposed empirical model as defined in Equation (1). In order to determine the parameters, which fit Equation (1) best, we utilized 'singular value decomposition' (SVD). The SVD technique is a powerful tool for diagnosis and solution of a problem involving multiple equations or matrices that are either singular or numerically very close to being singular. It is also the method of choice for solving the linear least-squares problem for parametric modeling of data [14]. It has been used for various other purposes like measurement locations for dynamic testing [15], treatment of ill-conditioning arising in spatial parameter estimation from measured vibration data [16] and to detect damage in structures under different operational conditions. The proposed empirical model can be represented as a linear system of equations. For example, the failure stress of specimen without prior exposure to environmental degradation can be expressed as,

$$S = c_1 + c_2 f + c_3 f^2. \tag{3}$$

When a specimen is exposed to both UV radiation and condensation, its failure stress can be represented as,

$$S = c_1(1+a) + c_2(1+b)\, f + c_3 f^2. \tag{4}$$

All 16 data can be expressed in a matrix form as, $\boldsymbol{S} = \boldsymbol{Fc}$. Here the matrix $\boldsymbol{F}$ contains corresponding amplitudes of cyclic load *f*, the vector $\boldsymbol{c}$ contains the unknown parameters (i.e., c_1, c_2, a_U, a_C, etc.), and the failure stresses are included in the vector $\boldsymbol{S}$. The SVD method computes $\boldsymbol{F}^+$, which is the generalized inverse of $\boldsymbol{F}$ (i.e., $\boldsymbol{FF}^+ = \boldsymbol{I}$, where $\boldsymbol{F}$ is not a square matrix). Once $\boldsymbol{F}^+$ is obtained, the unknown vector $\boldsymbol{c}$ can be solved as $\boldsymbol{c} = \boldsymbol{F}^+\boldsymbol{S}$. The generalized inverse is computed using the routine available in the IMSL software [17]. The computed values of the parameters are listed in Table 4.

In order to further study the error sensitivity of the procedure in estimating the unknown parameters,

Table 4 Parameters of the empirical model estimated using singular value decomposition

$c_1 = 0.963 \pm 0.0193$	$c_2 = -0.367 \pm 0.0036$	$c_3 = -0.059 \pm 0.0003$
$\alpha_U = -0.107 \pm 0.0013$	$\alpha_C = -0.156 \pm 0.0036$	$\alpha_{UC} = -0.191 \pm 0.004$
$\beta_U = -0.316 \pm 0.0060$	$\beta_C = -0.530 \pm 0.0037$	$\beta_{UC} = -0.586 \pm 0.0018$

Error ranges are obtained from sensitivity analysis based on the results in Table 3

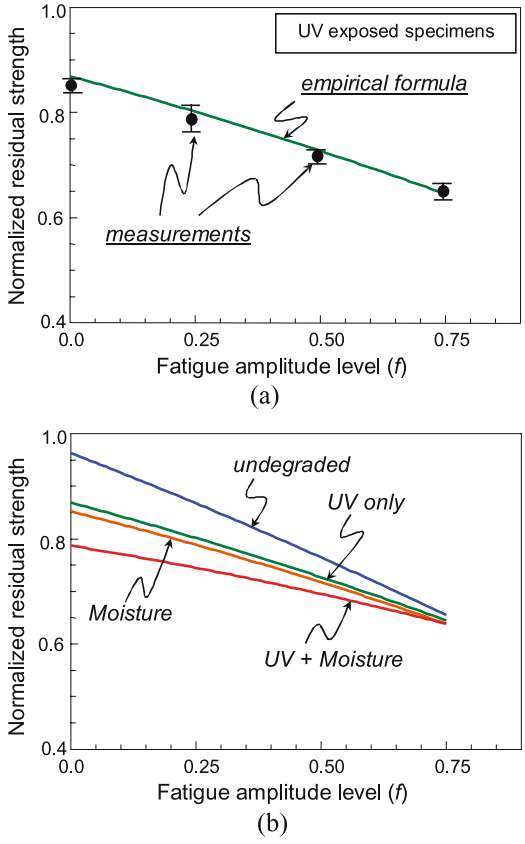

Fig. 8. (**a**) Comparison between experimental measurements and empirical model is shown for residual flexural strengths under various fatigue load amplitudes. (**b**) Decreasing residual strengths are shown for various environmental exposures according to empirical model

from the error bound of the failure moments shown in Table 3, multiple test runs were analyzed for different combinations of slightly altered failure moments. In each case, the values were modified by randomly selecting the error magnitudes. Based on 15 separate cases, it was found that the maximum variation in these parameters to be about 2% as noted in Table 4. This sensitivity analysis confirms that the empirical formula with the parameters determined by the singular decomposition method is effective in estimating the flexural failure characteristics of composites under of these particular conditions.

The subscripts for a and b indicate cases for UV only, moisture only and combined UV and moisture. From these values it is now possible to identify the individual and synergistic effects of the various environmental exposure conditions and cyclic loading. For example, it can be observed that absolute magnitude of a_C is greater than that of a_U. This means that the degradation due to condensation is more severe than that due to only UV radiation, especially when cyclic loading is not present. When fatigue loading is also present it can be seen that the magnitude of b_C is greater than b_U. This implies that mechanical fatigue has a more deleterious effect on specimens exposed to UV radiation than those exposed to condensation.

Based on the computed values, the formula can now be plotted along with the experimentally measured values. Figure 8 shows a comparison between the experimental measurements and the empirical model for the specimen exposed to combined UV and condensation. It can be seen that a good fit is obtained between the curve and the measured data. The comparison among different degradation conditions is shown in Fig. 9 where all the exposure conditions are plotted. It is interesting to note that although the curves have different initial values at $f = 0$, they converge to a similar value at $f = 0.75$. At this fatigue load level, the failure stress of composite

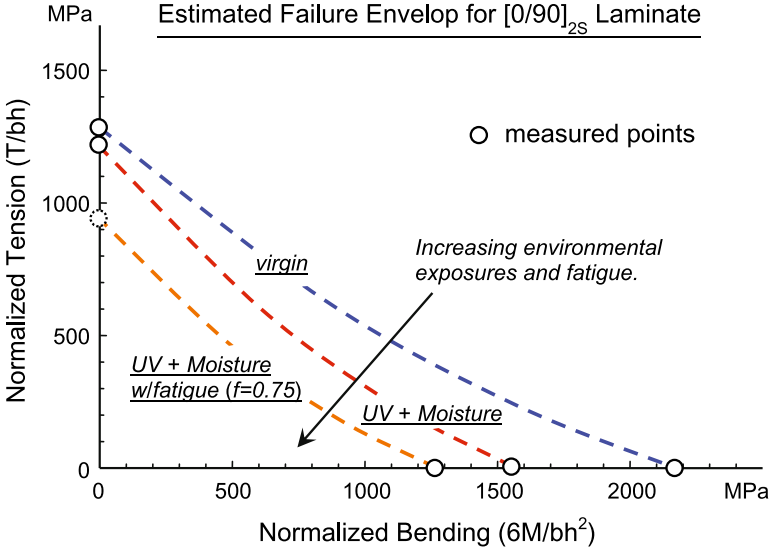

Fig. 9. Estimated failure envelops of cross-ply under combined tension and flexure. The schematic is only for illustrative purposes and actual measurements are only made under pure tension or bending

laminates is less than two-third of undegraded/non-fatigued specimen. The figure also clearly reveals an important aspect of environmental degradation. When a specimen is exposed to both UV radiation and condensation, its failure stress without any mechanical fatigue (at $f = 0$) is only 76% of virgin specimen. For an undegraded specimen, this value is only reached after 50,000 cycles at $f = 0.5$, which is a very high load level. Since, in general, composite structures are not designed to operate at such high load levels it is apparent that environmental effects can lead to severe deterioration of mechanical properties, much more than simply fatigue loading.

Conclusion

The mechanical response of carbon fiber reinforced composites exposed to various conditions of environmental degradation and fatigue loading were investigated in detail in order to allow better predictions of residual strength when these materials are subjected to multiple conditions of UV radiation, moisture condensation and cyclic loading. For the degraded specimens, synergistic mechanisms lead to extensive matrix erosion and microcracking, in addition to making the matrix brittle, thereby rendering the matrix structurally weak. Hence, degraded specimens showed an increased reduction in residual modulus than undegraded specimens for a given fatigue loading level. Amongst the various degradation conditions, a greater number of transverse cracks was observed for the moisture degraded specimens as compared to the UV degraded specimens. In case of specimens exposed to a combination of UV radiation and moisture condensation, the transverse cracks could not be distinguished due to matrix erosion. In order to quantify the synergistic effects of fatigue loading and the various exposure conditions residual strength tests were performed on the specimens. These tests indicated that at higher fatigue load levels, the effects of the various degradation conditions could be clearly distinguished. A decreasing trend in the failure strength was observed for all the different exposure conditions with an increase in the fatigue load level. The failure strength was the lowest for specimens exposed to combined UV radiation and moisture condensation. Unfortunately, the visual damage inspections of specimens by SEM were limited to free surfaces. Specimens were not cross-sectioned since that would introduce damages. Other means to qualify internal damage modes are under investigation.

Based on the residual strength measurements, an empirical relationship was formulated to develop a correlation between the synergism of fatigue and the degradation conditions. Singular value decomposition was used to extract the unknown parameters and a good correlation was obtained. This empirical formulation allowed for quantification of degradation effects in the current study. Most importantly it clarified that environmental effects could lead to severe deterioration of mechanical properties. For example, the failure stress of a composite degraded by exposure to both combined UV radiation and condensation without any cyclic loading is equivalent to subjecting an undegraded composite for 50,000 cycles of mechanical fatigue at 50% of its UTS. It is expected that the deleterious effect under flexure can occur even with a small bending in primary tensile condition. In order to illustrate the failure stresses under combined loading conditions, a failure enveloped is constructed as shown in Fig. 9. It is emphasized that this is an *estimated* illustration as only pure bending and tensile failure load results are available. Here measured failure loads are converted into corresponding stresses under tension and bending. The purpose of this illustration is to show that the failure envelop clearly shrinks as the environmental degradation and mechanical fatigue are imposed. Alternatively, the residual strength can be reduced significantly. An appropriate testing is being set up to actually quantify the remaining strength under combined loading.

Due to experimental difficulty and limitations, only two specimens were tested for each type of degradation and cyclic load condition. This was because the degrading of specimens by UV radiation and moisture condensation takes up to 45 days, and furthermore, the cyclic loading can be applied to only one specimen per day in the tensile machine. Here, combinations of various conditions totaled fifteen, excluding the undegraded and non-fatigued condition. The small number of specimens in each condition may pose some statistical unreliability; especially in the case of failure test data where variations are can be large in general. However, we note that the spreads in two results were generally low as shown in Table 3, and more significantly, the collections of *data variations* among all conditions were *consistent* (e.g., decreasing values as $f = 0 \rightarrow 0.75$). Thus, although two data points for each condition might not be sufficient, based on the data from all 32 specimens, the present results showed sufficient accuracy. Currently more specimens are being prepared and tested to confirm our results.

Acknowledgments This project is supported by the National Science Foundation under Grant No. CMS 0219250 and the U.S. Army Research Office under grant number DAAD19-02-1-0333. We are also thankful to Mr. Joe Morris of Cytec Engineered Materials (Anaheim, CA) for donating IM7/997 composite laminates.

References

1. Weitsman YJ (1991) Fatigue of Composite Materials. Elsevier, New York.
2. Jones FR (1999) Reinforced Plastics Durability. Woodhead Publishing Company, Cambridge, UK.
3. Zheng Q, Morgan RJ (1993) Synergistic thermal-moisture damage mechanisms of epoxies and their carbon-fiber composites. J Compos Mater 27(15):1465.
4. Adams RD, Singh MM (1996) The dynamic properties of fiber-reinforced polymers exposed to hot, wet conditions. Compos Sci Technol 56(8):977.
5. Zhao SX, Gaedke M (1996) Moisture effects on mode II delamination behavior of carbon/epoxy composites. Adv Compos Mater 5(4):291.
6. Choi HS, Ahn KJ, Nam JD, Chun HJ (2001) Hygroscopic aspects of epoxy/carbon fiber composite laminates in aircraft environments. Compos Part A Appl Sci Manuf 32(5):709.
7. Kumar BG, Singh RP, Nakamura T (2002) Degradation of carbon fiber reinforced epoxy composites by ultraviolet radiation and condensation. J Compos Mater 36(24):2713.
8. Gamstedt EK, Andersen SI (2001) Fatigue degradation and failure of rotating composite structures–material characterization and underlying mechanisms. Riso National Laboratory, Denmark.
9. Whitworth HA (1998) A stiffness degradation model for composite laminates under fatigue loading. Compos Struct 40(2):95.
10. Reifnsnider K (1980) Fatigue behavior of composite materials. Int J Fract 16(6):63.
11. Morris J (2001) Private communication. Cytec-Fiberite, Inc., Anaheim, California.
12. ASTM D3479/D3479M (1996) Standard test method for tension-tension fatigue of polymer matrix composite materials. American Society for Testing and Materials, West Conshohocken, PA.
13. Salkind MJ (1972) In: Composite materials: testing and design ASTM. STP 497, American Society of Testing and Materials, Philadelphia, PA, p. 143.
14. Teukolsky SA, Vetterling, WT, Flannery BP (1992) Numerical Recipes in C: The Art of Scientific Computing. Cambridge University Press, Cambridge, UK.
15. Penny JET, Friswell MI, Garvey SD (1994) Automatic choice of measurement locations for dynamic testing. AIAA J 32:407.
16. Mottershead JE, Foster CD (1991) On the treatment of Ill-conditioning in spatial parameter estimation from measured vibration data. Mech Syst Signal Process 5:139.
17. IMSL Mathematical and Statistical Libraries (1999) Visual Numerics, Inc., San Ramon, CA.